Supporting Information for Plasmonic Enhancement of Two-Photon-Excited Luminescence of Single Quantum Dots by Individual Gold Nanorods

Weichun Zhang, Martín Caldarola, Xuxing Lu, Michel Orrit*

Huygens-Kamerlingh Onnes Laboratory, Leiden University, 2300 RA Leiden, Netherlands

*Email: orrit@physics.leidenuniv.nl

Contents

Schematic of the experimental setup

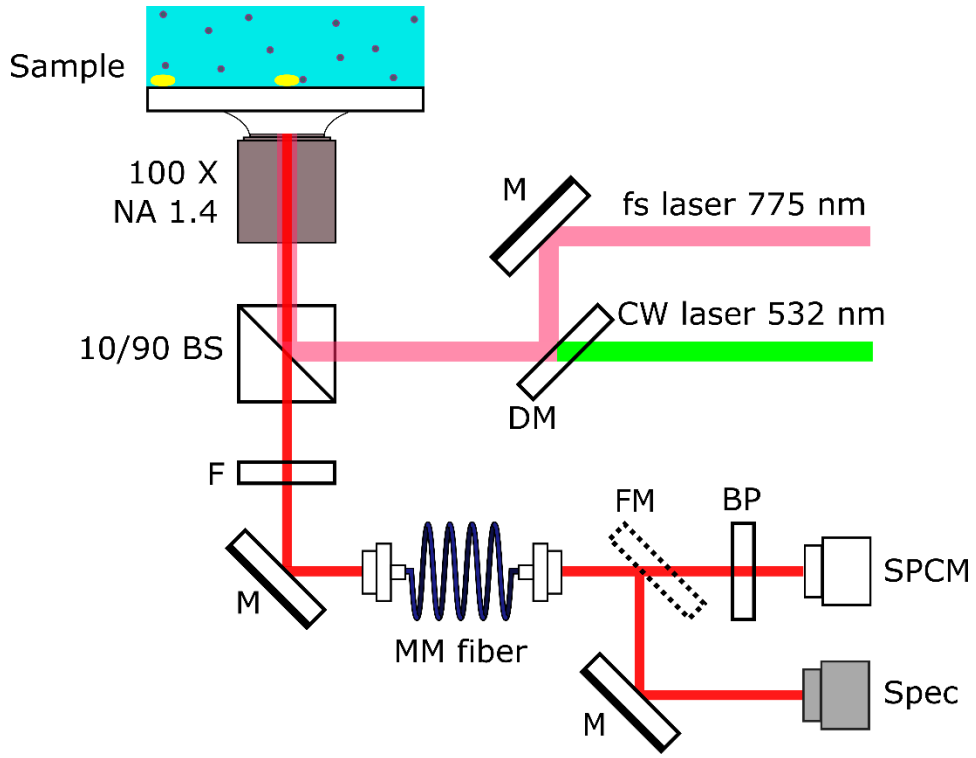

Figure S1. Schematic of the experimental setup for two-photon microscopy and luminescence spectra measurements. BS – beam splitter, F – Set of filters: 745 nm short-pass filter + 785 notch filters for the Ti:Sapphire laser or two 532 nm notch filters for the 532-nm laser, M – mirror, DM – dichroic mirror, FM – flip mirror, BP – bandpass filter, MM fiber – multimode fiber, SPCM – single-photon counting module, Spec – spectrometer. Waveplates and spatial filters are not shown in the scheme.

Two-photon fluorescence microscopy measurements were performed on our home-built sample-scanning confocal fluorescence microscope (Figure S1). A mode-locked Ti:Sapphire laser (Coherent Mira 900) was made circularly polarized by a quarter-wave plate (not shown in the scheme) before entering the oil immersion objective (100×, NA=1.4, Zeiss), and used for two-photon excitation. It was spatially filtered and expanded to overfill the aperture of the objective. The laser operated at 775 nm, 76 MHz repetition rate and ~220 fs pulse width. The two-photon excited photoluminescence signal of QDs and/or GNRs collected by the same objective was filtered out from the back scattered excitation light by a 745-nm short-pass filter (FF01-745/SP-25, Semrock) and a 785-nm notch filter (NF03-785E-25, Semrock). A multimode optical fiber with a core size of 62 μm was used as a confocal pinhole. In principle, two-photon microscopy does not require a pinhole, but the optical fiber efficiently lowers the background from stray light. After gold nanorods were found by raster scanning (Figure S1), a 650-nm bandpass filter (HQ650/50, Chroma) was used to reduce the background from multi-photon photoluminescence of nanorods when recording time traces.

A 532-nm diode-laser-pumped solid-state continuous-wave laser (Shanghai Laser & Optics Century Co., Ltd), which matches the transverse plasmon resonance of nanorods, was used to measure the one-photon excited photoluminescence spectrum of each nanorod. For this, two 532-nm notch filters were used in place of the 745-nm shortpass and 785-nm notch filters. We used circular polarization to find nanorods regardless of their orientation. It was previously shown that nanorods' one-photon photoluminescence spectra closely resemble their scattering spectra[11], so photoluminescence is used to determine the resonance wavelengths. The near-infrared and green laser beams were overlapped with a shortpass dichroic mirror (FF720-SDi01-25x36, Semrock). Note that the two lasers were not used at the same time. We used a motorized flip mirror to direct luminescence either to a single-photon counting module (SPCM-AQR-16, PerkinElmer) or to a spectrometer equipped with a liquid-nitrogen-cooled CCD (Acton SP-500i, Princeton Instruments). The raw spectra are corrected by taking into account the wavelength-dependent detection efficiency of the setup (Figure S3).

Images of gold nanorods were obtained by scanning the sample with a 3-axis piezostage (Physik Instrumente) controlled by a data acquisition card (ADWin Gold, Germany) and a home-written Python program. Timetraces were recorded with a time-correlated single-photon counting (TCSPC) module (Timeharp 200, PicoQuant GmbH, Berlin). The single-photon data were analyzed with SymPhoTime software (PicoQuant GmbH, Berlin).

Photoluminescence image of nanorods

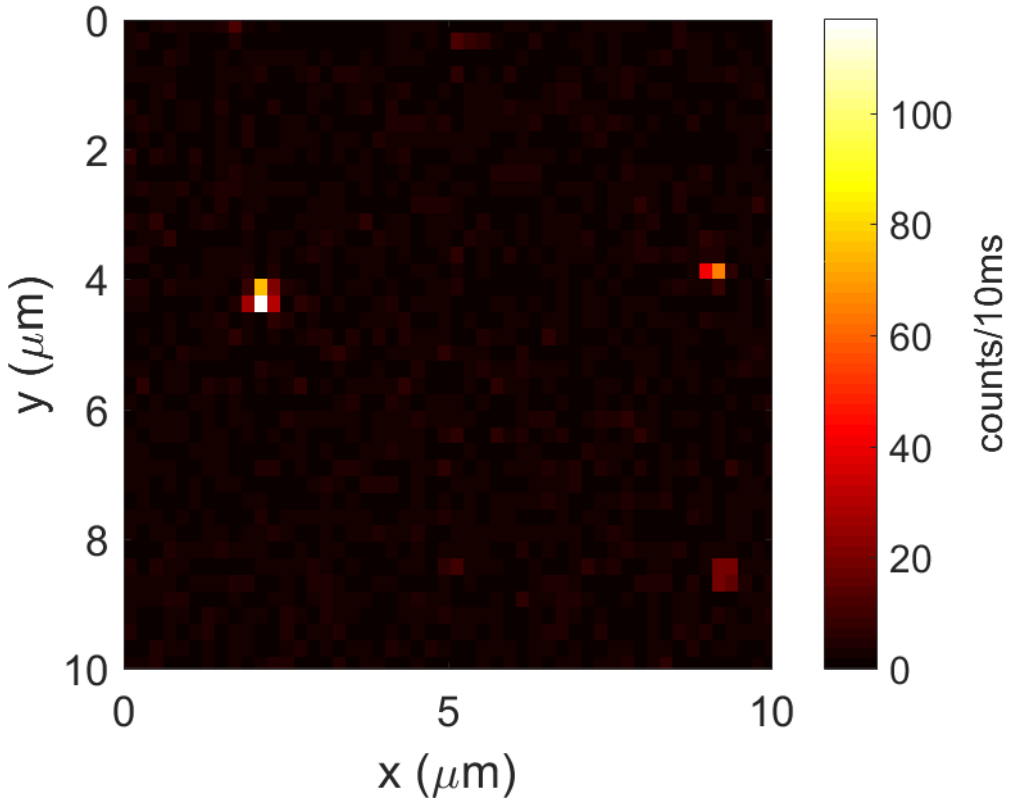

Figure S2. A typical luminescence raster scan image of gold nanorods immersed in water containing 150 nM QDs. The image has 50 × 50 pixels with an integration time of 10 ms/pixel. The average power of the fs excitation laser at the sample was 1.55 kW/cm^2. The 650-nm bandpass filter was absent for this image.

Gold nanorods in our study were purchased from Nanopartz Inc. (A12-40-780-CTAB). The average size was 38 nm × 118 nm by diameter and length according to the manufacturer. Individual isolated gold nanorods were immobilized on a glass coverslip by spin coating. The detailed procedure was described elsewhere[12]. Figure S2 shows an example PL image of the sample excited with the fs laser.

Relative detection efficiency of the setup and corrected photoluminescence spectra of nanorods

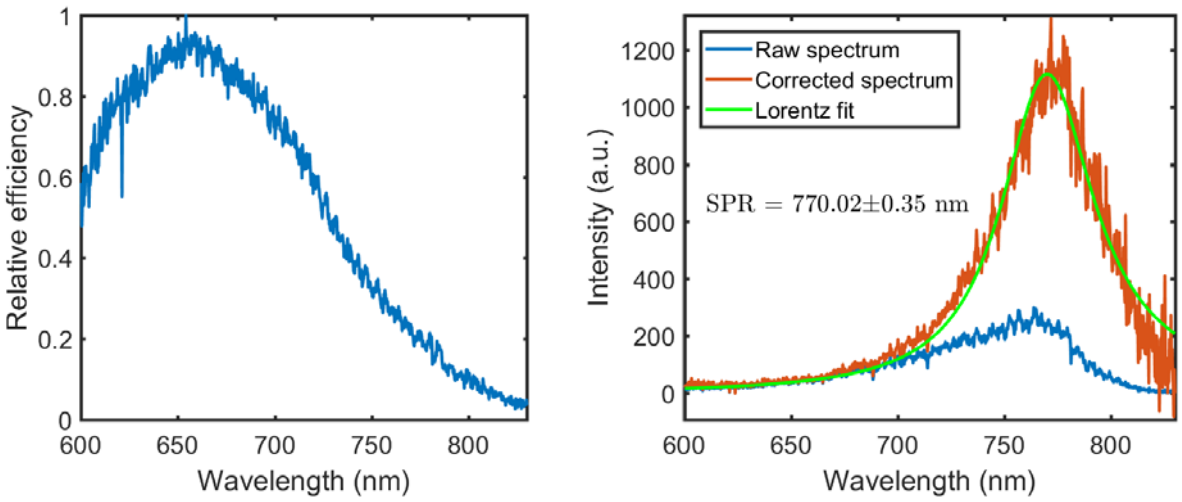

Figure S3. Left: Relative detection efficiency of the setup as a function of wavelength. (Right) The one-photon photoluminescence raw (blue) and corrected (red) spectra of a single nanorod. The corrected spectrum was fitted with Lorentzian line shape (green), yielding a resonance wavelength of 770.02 ± 0.35 nm.

The spectra of gold nanorods are in the near-infrared range, where the detection efficiency of the setup is poor. Therefore, the measured raw spectra have to be normalized by the spectral response of the setup.

An emission standard dye for the near-infrared range, 4-dimethylamino-4'-nitrostilbene (4,4'-DMANS, Sigma-Aldrich), was excited with the same excitation laser. The wavelength-dependent relative detection efficiency was obtained by normalizing the measured fluorescence spectrum by the real emission spectrum of the standard dye.[3] The measured spectra of nanorods, with the background spectra subtracted, were corrected for the detection efficiency function and further fitted with a Lorentzian profile to obtain the localized surface plasmon resonance wavelength. The right panel of Figure S3 shows an example spectrum of a single nanorod with spectral correction and Lorentzian fitting.

Two-photon-excited fluorescence correlation spectroscopy

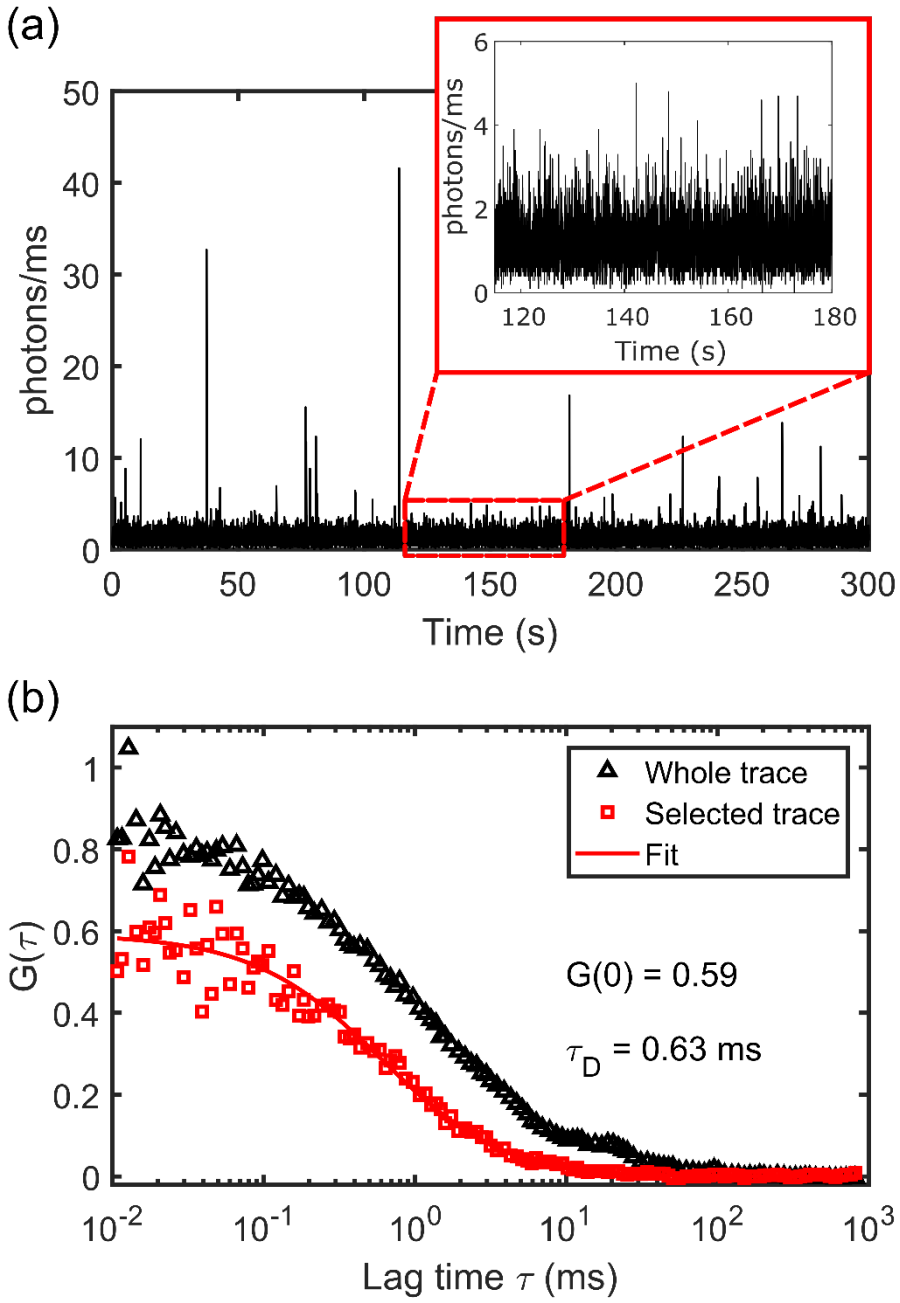

Figure S4. (a) Emission intensity time trace (binned to 10 ms) recorded from a solution of 30 nM QDs (λ_{em} = 655 nm) with 3 mM NaCl without gold nanorods. The high bursts evidence the presence of aggregates of QDs in the solution. The average excitation intensity was 15.5 kW/cm^2. The inset shows a zoom-in of the zone marked with the rectangle. This evidences the presence of single-QD bursts. (b) The black triangles plot the autocorrelation curve of the whole time trace shown in (a). The stretched longer component at up to 30 ms comes from the strong bursts in (a). The red squares show the autocorrelation for the photons within the marked window in (a). No strong bursts were present in this period of time trace. The autocorrelation curve can be fitted with a translational diffusion model, yielding an amplitude of 0.59 ± 0.02 and a diffusion time τ_D of (0.63 ± 0.07) ms.

To measure the average brightness of individual QDs without enhancement, we excite a solution of 30 nM QDs with 3 mM NaCl with a fs laser (average 15.5 kW/cm^2, circularly polarized). About 20 high bursts in 300 seconds can be observed (Figure S4 (a)), which cannot be explained by the intensity fluctuations due to single quantum dots diffusing in and out of the focal volume. They are probably a consequence of a small amount of large clusters of QDs present in the solution. The longer time component (≤30 ms) in the autocorrelation curve for the entire time trace (back triangles in Figure S4 (b)) is probably from the clusters, which diffuse slower than single QDs. We tried several separation and filtering methods to get rid of the clusters, but it appeared that these clusters always reform in the aqueous solution. By autocorrelating photons within a period of time without high bursts (marked by a red box in Figure S4 (a)), we got the autocorrelation curve for single quantum dots, which is shown as red triangles in Figure S4 (b). The autocorrelation curve was fitted with the following diffusion model[6, 7]

$$G(\tau) = G(0)\frac{1}{1+\tau/\tau_D}\frac{1}{\left[1+\left(w_0/z_0\right)^2\tau/\tau_D\right]^{1/2}},$$

where w_0 and z_0 are the $1/e^2$ width along the radial and axial direction of the excitation volume, respectively and τ_D is the diffusion time. For the fitting we used the values $w_0 = (202 \pm 2)$ nm and $z_0 = (560 \pm 5)$ nm ($V_{conf} = 3 \times 10^{-2}$ fL). The fitting result is shown as a solid red line in Figure S4 (b). The number of QDs contributing to the average photoluminescence signal (1130.7 ± 28.2 counts/s) is related to the fitted amplitude of the autocorrelation function ($G(0)$) through $N = \gamma / G(0)$, where γ is geometrical factor that accounts for the shape of the excitation profile. For an overfilled objective lens, the excitation profile is a 3D-Gaussian and $\gamma = 2^{-3/2}$ (ref. 7), therefore we obtained N = 0.60 ± 0.02, which means a two-photon-excited confocal volume of (0.03 ± 0.01) fL. Then the brightness of each QD was calculated to be 1890 ± 70 counts/s at 15.5 kW/cm^2.

By considering the quadratic emission-intensity relation of two-photon photoluminescence, we found that the average brightness of each QD at the intensity used for the enhancement experiments (1.55 kW/cm^2 at the center of the excitation volume) should be 19.0 ± 0.7 counts/s. The excitation intensity was well below saturation. We found no evidence of blinking on microsecond to millisecond time scales, which is in agreement with previous observations[4, 13]. The study by Yao et. al. suggests that QDs are still blinking in solution but longer dwell times are needed to detect the blinking.[10]

Blank experiments

We performed some blank experiments to confirm that the luminescence signal observed was indeed coming from the QDs and not from some other chemical species in the solution. First, we measured under the same experimental conditions (low excitation intensity) used for the enhanced experiment in a position far away from any nanorod. The obtained time trace in this case is shown in Figure S5 (a) with an inset representing the position of the laser spot away from the nanorod but in presence of the QDs. No bursts are observed. Note that the quantum dots are diffusing during the experiment and that at this extremely low power the two-photon excitation does not provide much signal.

Second, we measured luminescence in the same experimental conditions used for the enhancement but in a solution without any QDs on top of a nanorod. The measured time trace for this case is shown in Figure S5 (b) with an inset showing the scheme of the experiment. Again, there are not bursts, as expected, but there is a significant signal that we assign to two-photon-excited photoluminescence of the gold nanorods. This is a quite efficient process since the laser is hitting the surface plasmon resonance of the particle and thus the absorption cross section is remarkably high.

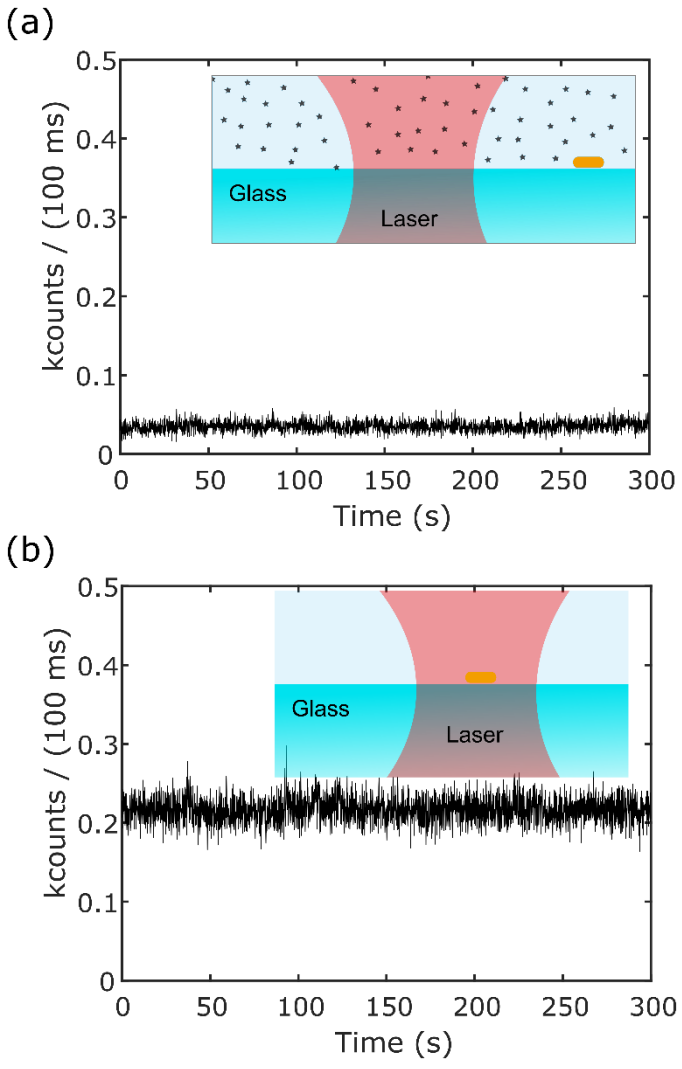

Figure S5. (a) A time trace recorded on a solution of 30 nM QD and 3 mM NaCl in water, with no gold nanorod present. (b) A time trace taken on a single gold nanorod in 3 mM NaCl, with no QD present. In both experiments, the excitation conditions were the same as in the enhancement experiment (Figure 2 in the main text).

QD concentration dependence

We also studied the concentration dependence of the enhanced signal from single QDs. We observed an approximate 5 times increase in the number of events registered in 275 s when we increase the concentration by a factor of 5.

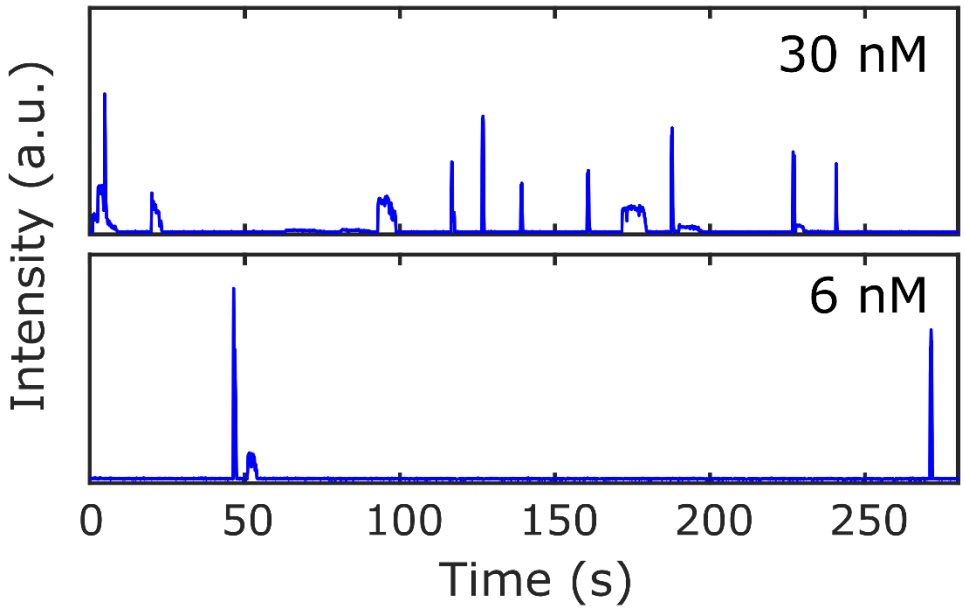

Figure S6. Timetraces recorded on the same gold nanorod at two different QD concentrations (6 nM and 30 nM). The timetrace for 30 nM is shifted for clarity. The excitation is 1.55 kW/cm^2 at 775 nm.

One-photon-excited luminescence decay of Qdot 655

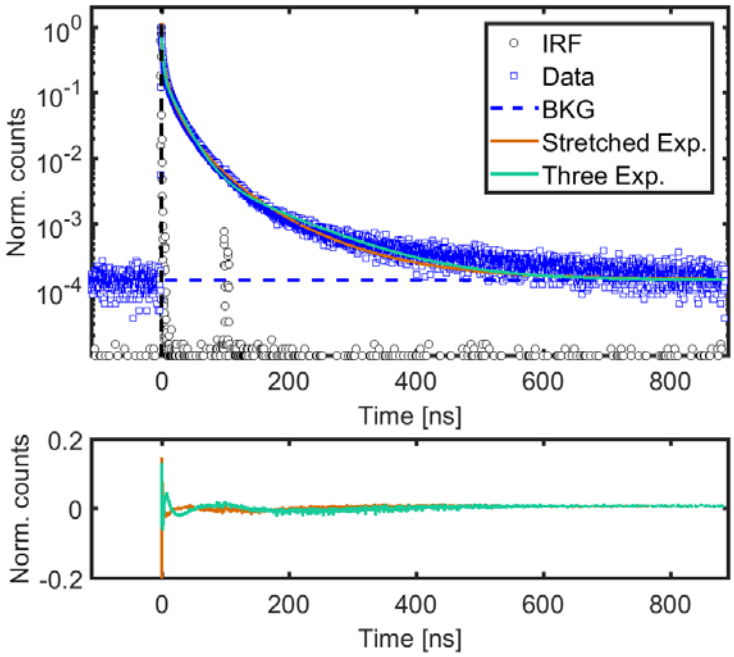

Figure S7. One-photon-excited luminescence decay curve of a solution of Qdot 655 in water (150 nM). Top: decay data from QDs (blue squares) and IRF (black circles). The vertical dashed line shows t=0 s while the horizontal dashed line represents the background signal. The fits for stretched exponential and three exponentials are also shown. Bottom: residuals from the fits with the same color code used on top.

To measure the complete luminescence decay, an aqueous solution of 150 nM Qdot 655 and 3 mM NaCl was excited by a picosecond diode laser (Power Technology, Little Rock, AR, USA) with a wavelength of 635 nm and a repetition rate of 1 MHz. The emission was detected by an avalanche photodiode (SPCM AQRH-15, Perkin Elmer Inc., USA) and counted by a TCSPC card (PicoHarp 300, PicoQuant GmbH, Berlin, Germany). Figure S7 at the top shows the PL decay of the sample over a time window of 1 µs, along with the impulse response function of our system. We observe a non-exponential decay, commonly reported in the literature for quantum dots and usually attributed to the size distribution,[2, 5] blinking and environmental fluctuations.[1, 8, 9]

In order to model this behavior we used a stretched exponential[8]

$$f(\tau) = A \exp\left[\left(-\frac{\tau}{\tau_0}\right)^{\beta}\right]$$

and, alternatively, a sum of three exponentials

$$g(\tau) = w_1 e^{-\tau/\tau_1} + w_2 e^{-\tau/\tau_2} + (1 - w_1 - w_2) e^{-\tau/\tau_3}$$

to fit the decay. We also show both fits in Figure S7. For the stretched exponential we obtained a τ_0 =1.51 ns and an exponent β = 0.39, while for the three exponentials we obtained τ_1 = 1.5 ns ($w_1 = 66.92$ %), τ_2 = 16.5 ns ($w_2 = 25.06$ %), τ_3 = 46.2 ns ($w_3 = 8.02$ %). Note that our curves are normalized to get a unity value at zero time and the percentage amplitudes in brackets correspond to the percentage weight of each exponential.

For the stretched exponential model, we calculated the average lifetime by [8]

$$\langle \tau \rangle = \frac{\tau_0}{\beta} \Gamma\left(\frac{1}{\beta}\right) = 5.09 \text{ ns}$$

where Γ represents the gamma function.

For the three-exponential model, we calculated different probabilities of the three QD forms according to the two models presented in the main text.

In model 1 presented in the main text, the probabilities of the three forms are just proportional to the initial fluorescence intensity w_i, because their radiative rate is identical and thus initial intensities are proportional to the number of QDs. Thus we obtained an amplitude-weighted average lifetime of 8.88 ns by

$$\langle \tau_{\text{amp}} \rangle = \sum_i w_i \tau_i$$

In model 2, because the quantum yield is the same for all three populations of QDs, these populations are proportional to the total number of photons emitted, corresponding to new weights $W_i = w_i \tau_i / \sum_j w_j \tau_j$. We obtained $W_1 = 11.54\%$, $W_2 = 46.68\%$, $W_3 = 41.78\%$. Thus, we obtained an intensity-weighted average lifetime of 27.2 ns by

$$\langle \tau_{\text{int}} \rangle = \sum_i W_i \tau_i$$

QDs quantum yield.

We measured the ensemble quantum yield (QY) of the quantum dots using a fluorimeter and obtained 0.80 ± 0.05. The quantum yield η_i of each component i is

$$\eta_i = \frac{k_{ri}}{k_{ri} + k_{nri}} = \tau_i k_{ri}$$

where k_r and k_{nr} represents the radiative and non-radiative rates and τ_i is the lifetime for each component.

For model 1, with $\eta_3 = 1$ we can calculate the average quantum yield as

$$\langle \eta \rangle = \sum_i w_i \eta_i,$$

and obtained a value of $\langle \eta \rangle = 0.19$. For the model 2, the average quantum yield is obviously unity. Thus, the two extreme models give upper and lower bounds to the expected experimental values.

Excitation saturation

We performed a power dependence study of the collected luminescence of a solution of QD in the same conditions as the enhancement experiment. This time we increased the excitation intensity until we found the saturation value. We find that the saturation occurs at ~3000 kW/cm^2. For our enhancement experiments, we use an intensity of 1.55 kW/cm^2, which is ~2000 times smaller than the saturation value. The nanorods provide a maximum intensity enhancement of × 1200 for linearly polarized light (× 600 for circularly polarized light, as shown in Figure 3 in the main text) at their tips, so a QD sitting close to the tip will see an intensity at most 1200 times higher than the excitation intensity, which is still below the saturation value.

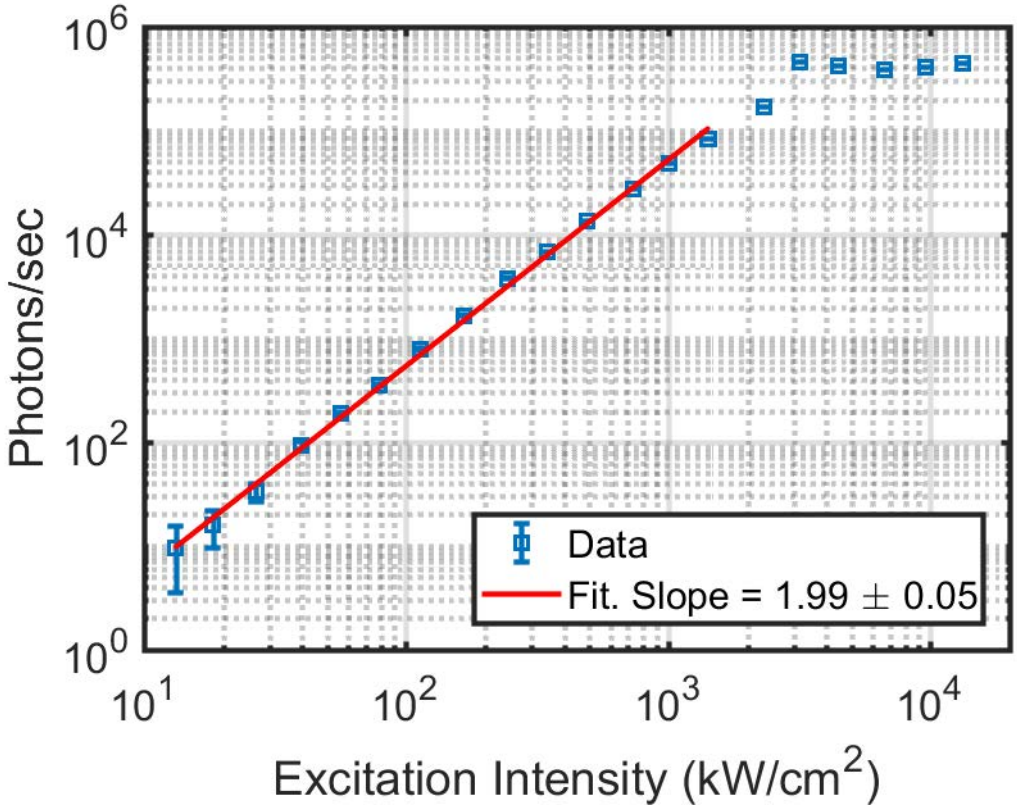

Figure S8. Two-photon-excited photoluminescence signal from an aqueous solution of Qdot 655 doped with 3 mM NaCl as a function of the excitation intensity at the center of the focused excitation volume. The curve deviates from the intensity-square relation at high intensities, indicating an excitation saturation threshold of ~3000 kW/cm^2.

Burst analysis: correlation between duration and intensity

We analyzed the two-photon-excited enhanced time trace shown in Figure S9 (a) to extract the burst duration and the intensity of each enhancement event and plotted the burst duration as a function of the intensity observed during the burst. Figure S9 (b) shows the correlation plot between these two quantities in linear scale and (c) in log-log scale. We see that the high-intensity bursts have a short duration and that bursts with low intensity usually last longer.

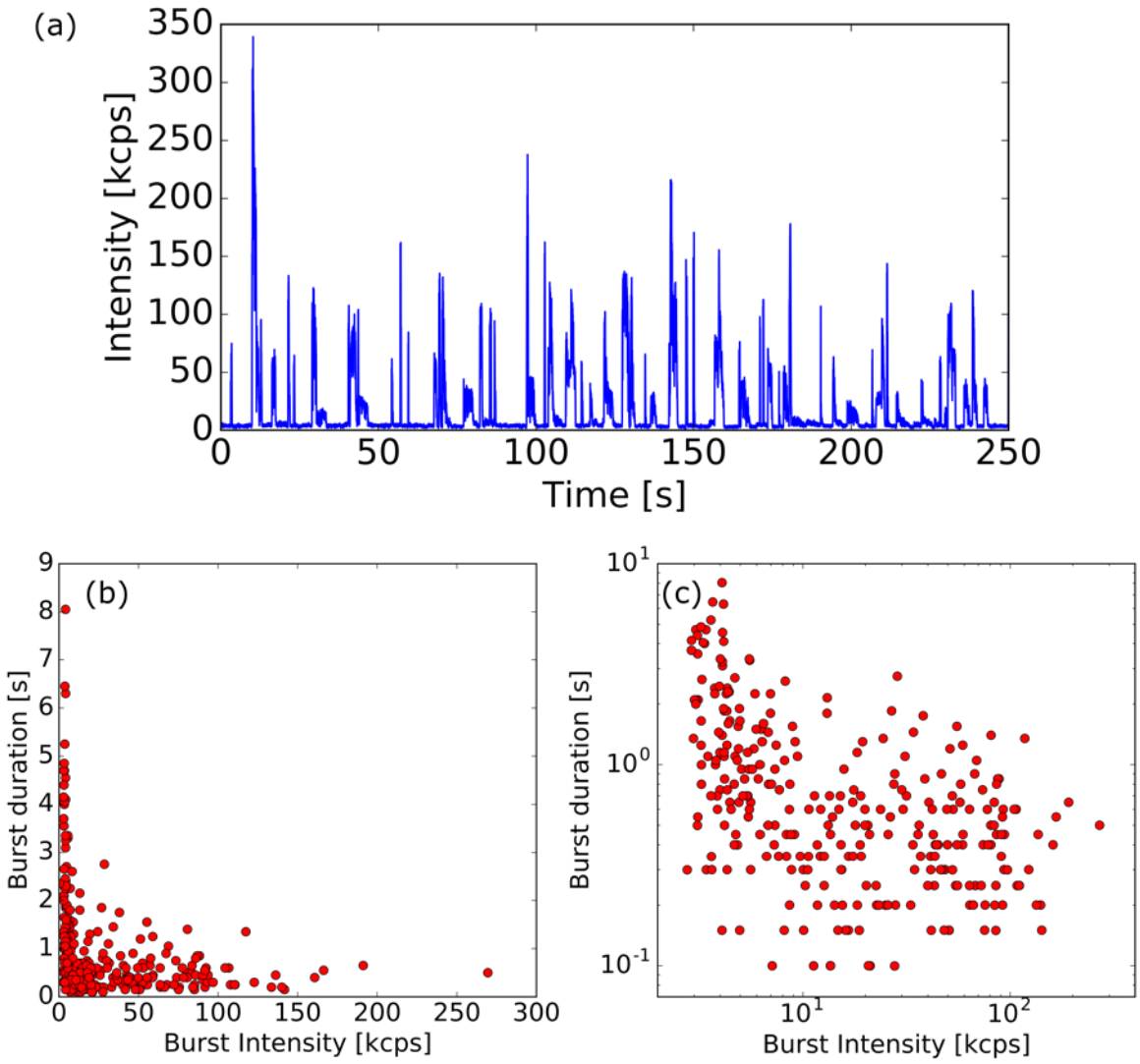

Figure S9. (a) Two-photon-excited photoluminescence enhanced time trace of Qdot 655. (b) Linear scale plot of the burst duration as a function of the burst intensity. (c) Same plot as (b) in log-log scale.

Quantum dots structure

For our study we used commercial quantum dots from Invitrogen (Qdot 655 ITK amino-PEG). They have a core-shell structure of CdSe/ZnS with a rod-like shape. The length and width are 12 nm and 7 nm, respectively, giving an aspect ratio of 1.71. It is further coated with an amphiphilic polymer shell to enable conjugation of amine-derivatized polyethylene glycol (PEG). Figure S10 shows a scheme of the QDs. The last layer of PEG-amine is about 2 nm thick.

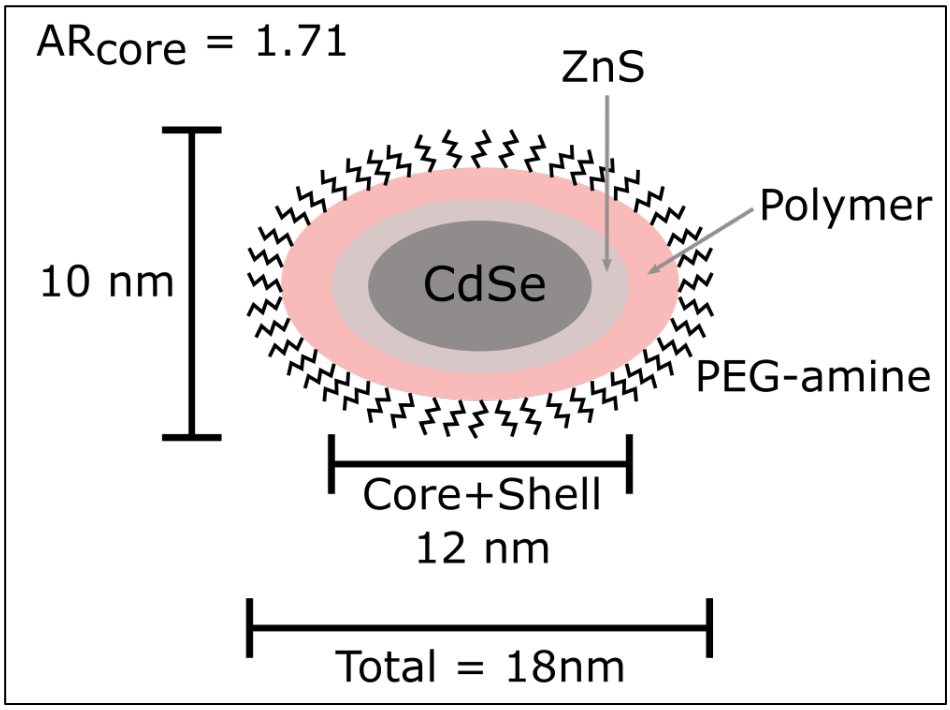

Figure S10. Scheme of the QDs used for the study.

Enhancement time traces at different NaCl concentration

We took traces at different concentration of NaCl to empirically obtain the optimum concentration for our study. We seek a situation where we have clearly distinguished enhancement events, sparse enough in time to address them individually. Figure S11 shows two time traces, the top one at 1mM and the bottom one at 5 mM concentration of NaCl. We see that when the concentration is too high, the enhancement events overlap in time, complicating the analysis..

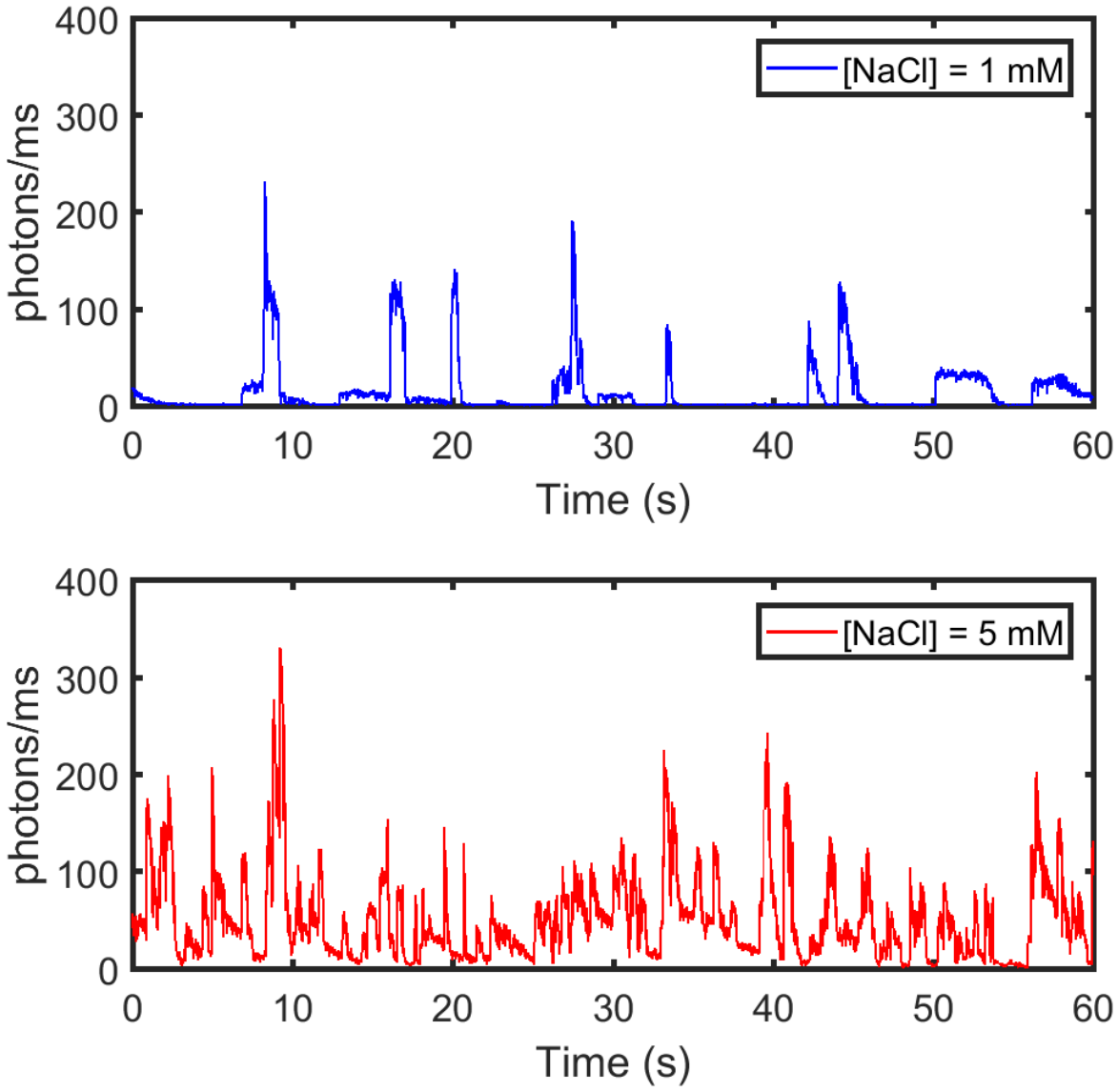

Figure S11: Enhanced time traces of QDs by gold nanorods at different concentrations of NaCl. Top 1 mM, bottom 5mM.

Effect of finite size of the QD

In order to take into account the finite size of the QD we averaged the near-field map over the dimensions of the QD core. Figure S12 (a) shows a scheme for the two situations taken into account: the quantum dot oriented along the longitudinal axis of the nanorod (x) and along the transverse axis (y). Figure S12 (b) shows the resulting curves with the presented notation. The point dipole approximation gives rise to an error smaller than 20 % in all cases.

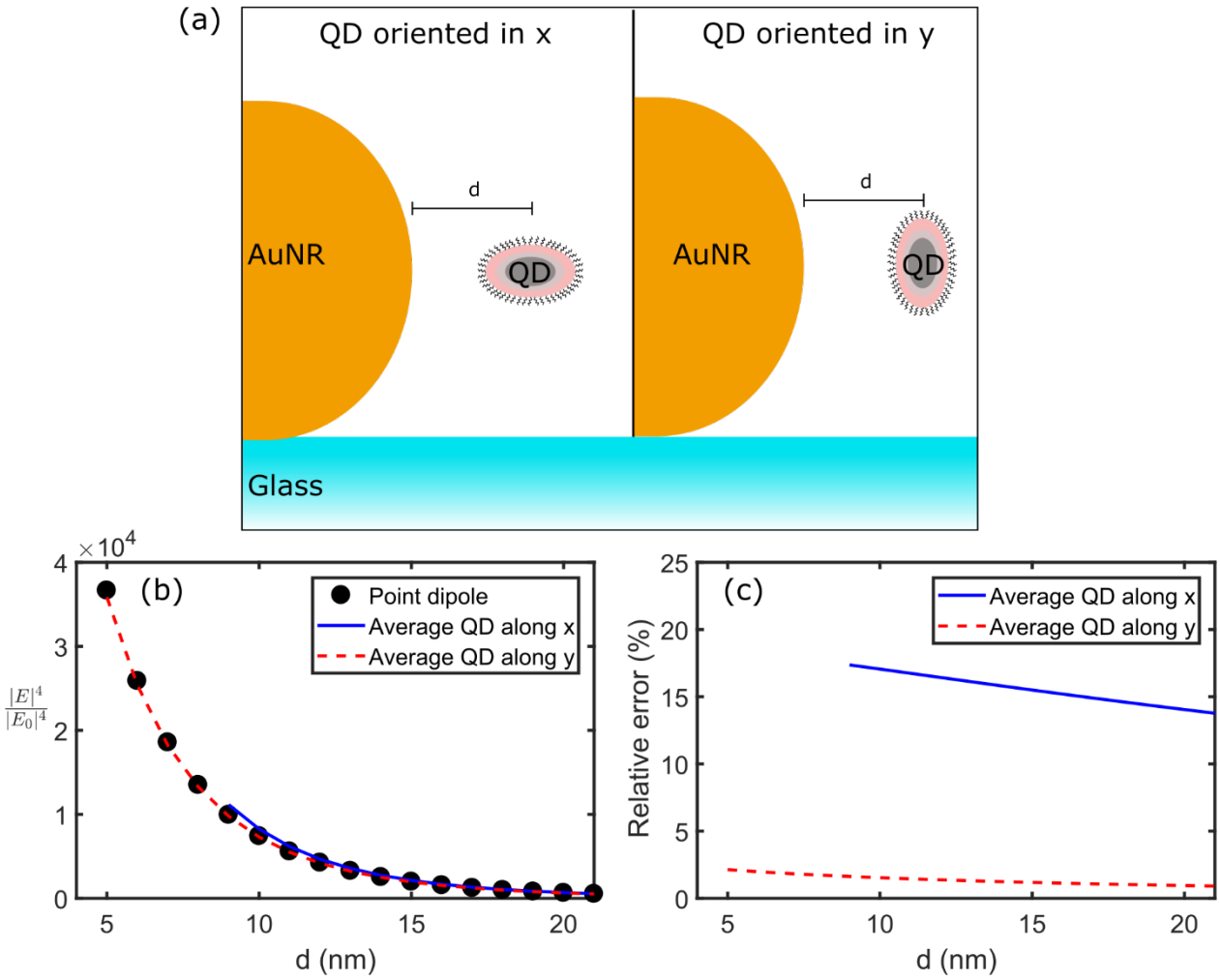

Figure S12: (a) Scheme of the average procedure. (b) Excitation enhancement for a point dipole and the averaged values for the two situations described on top. (c) Relative error

References

1 Nicole Amecke, and Frank Cichos, 'Intermediate Intensity Levels During the Emission Intermittency of Single Cdse/Zns Quantum Dots', *Journal of luminescence*, 131 (2011), 375-78.

2 Brent R. Fisher, Hans-Jürgen Eisler, Nathan E. Stott, and Moungi G. Bawendi, 'Emission Intensity Dependence and Single-Exponential Behavior in Single Colloidal Quantum Dot Fluorescence Lifetimes', *The Journal of Physical Chemistry B*, 108 (2004), 143-48.

3 Joseph R. Lakowicz, *Principles of Fluorescence Spectroscopy*. 3 edn (Springer US, 2006), p. 954.

4 Daniel R. Larson, Warren R. Zipfel, Rebecca M. Williams, Stephen W. Clark, Marcel P. Bruchez, Frank W. Wise, and Watt W. Webb, 'Water-Soluble Quantum Dots for Multiphoton Fluorescence Imaging in Vivo', *Science*, 300 (2003), 1434-36.

5 Xuedan Ma, Hua Tan, Tobias Kipp, and Alf Mews, 'Fluorescence Enhancement, Blinking Suppression, and Gray States of Individual Semiconductor Nanocrystals Close to Gold Nanoparticles', *Nano Letters*, 10 (2010), 4166-74.

6 Michele Marrocco, 'Two-Photon Excitation Fluorescence Correlation Spectroscopy of Diffusion for Gaussian− Lorentzian Volumes', *The Journal of Physical Chemistry A*, 112 (2008), 3831-36.

7 Attila Nagy, Jianrong Wu, and Keith M. Berland, 'Observation Volumes and Γ-Factors in Two-Photon Fluorescence Fluctuation Spectroscopy', *Biophysical Journal*, 89 (2005), 2077-90.

8 Germar Schlegel, Jolanta Bohnenberger, Inga Potapova, and Alf Mews, 'Fluorescence Decay Time of Single Semiconductor Nanocrystals', *Physical Review Letters*, 88 (2002), 137401.

9 PH Sher, JM Smith, PA Dalgarno, RJ Warburton, X Chen, PJ Dobson, SM Daniels, NL Pickett, and P O'Brien, 'Power Law Carrier Dynamics in Semiconductor Nanocrystals at Nanosecond Timescales', *Applied Physics Letters*, 92 (2008), 101111.

10 Jie Yao, Daniel R Larson, Harshad D Vishwasrao, Warren R Zipfel, and Watt W Webb, 'Blinking and Nonradiant Dark Fraction of Water-Soluble Quantum Dots in Aqueous Solution', *Proceedings of the National Academy of Sciences of the United States of America*, 102 (2005), 14284-89.

11 M. Yorulmaz, S. Khatua, P. Zijlstra, A. Gaiduk, and M. Orrit, 'Luminescence Quantum Yield of Single Gold Nanorods', *Nano Lett*, 12 (2012), 4385-91.

12 H. Yuan, S. Khatua, P. Zijlstra, M. Yorulmaz, and M. Orrit, 'Thousand-Fold Enhancement of Single-Molecule Fluorescence near a Single Gold Nanorod', *Angew Chem Int Ed Engl*, 52 (2013), 1217-21.

13 Eli Zamir, Piet H. M. Lommerse, Ali Kinkhabwala, Hernan E. Grecco, and Philippe I. H. Bastiaens, 'Fluorescence Fluctuations of Quantum-Dot Sensors Capture Intracellular Protein Interaction Dynamics', *Nat Meth*, 7 (2010), 295-98.